Yu Xu, Xiu-Jie Xu, Zhuang Li, Tao Wang, An-Yuan Deng and En-Gang Wang*

Dendrite Growth Characteristics and Segregation Control of Bearing Steel Billet with Rotational Electromagnetic Stirring

DOI 10.1515/htmp-2016-0128
Received June 26, 2016; accepted January 18, 2017

Abstract: The effects of rotational electromagnetic stirring (R-EMS) on dendrite growth characteristics and segregation control of bearing steel billet were investigated in continuous casting. The results show that applying R-EMS can promote columnar-equiaxed transition, increase the region of the equiaxed grain from 5 % to 45 %, decrease the secondary dendrite arm spacing (SDAS), and reduce the segregation of both carbon and sulfur. Meanwhile, the fragments of dendrite arms induced by R-EMS are observed. The length of the dendrite fragmentation is approximately 1.5 mm, 7–10 times the SDAS. Some fragments can partially remelt to become effective nuclei, and some fragments survive the solidification process.

Keywords: dendrite growth, bearing steel, rotational electromagnetic stirring, segregation

***Corresponding author: En-Gang Wang,** Key Laboratory of Electromagnetic Processing of Materials (Ministry of Education), Northeastern University, No. 3–11, Wenhua Road, Shenyang 110004, P. R. China; School of Metallurgy, Northeastern University, Shenyang 110004, P. R. China,
E-mail: egwang@mail.neu.edu.cn
Yu Xu, Xiu-Jie Xu, Key Laboratory of Electromagnetic Processing of Materials (Ministry of Education), Northeastern University, No. 3–11, Wenhua Road, Shenyang 110004, P. R. China; School of Metallurgy, Northeastern University, Shenyang 110004, P. R. China
Zhuang Li, Key Laboratory of Electromagnetic Processing of Materials (Ministry of Education), Northeastern University, No. 3–11, Wenhua Road, Shenyang 110004, P. R. China; School of Materials Science and Engineering, Northeastern University, Shenyang 110004, P. R. China
Tao Wang, An-Yuan Deng, Key Laboratory of Electromagnetic Processing of Materials (Ministry of Education), Northeastern University, No. 3–11, Wenhua Road, Shenyang 110004, P. R. China; School of Metallurgy, Northeastern University, Shenyang 110004, P. R. China

Introduction

The GCr15 bearing steel is widely applied in rail transportation and automobile industry because of its excellent mechanical properties [1]. However, high carbon steel tends to solidify over a wide temperature range, so the center segregation and porosity are the major problems during the continuous casting process of billet [2–4]. The solidifying dendrites reject dissolved elements continuously at the solidification front, due to less solubility of solutes in the solid phase as compared to liquid phase, thereby leading to gradual enrichment of remaining liquid and forming the segregation of solute elements [5]. Generally, the solidification style of liquid steel and dendrite morphology have remarkable effects on the quality of billet [6–8]. Dendrite growth characteristics are controlled by the mass and heat transfer process during solidification. Meanwhile, the dendritic solidification parameters, such as primary and secondary dendrite arm spacing, are important to predict the crack susceptibility of steel, and the permeability of the mushy zone, which is crucial to accurately investigate the formation and the development of central macrosegregation [9]. Furthermore, a small variation of the cooling rate or thermal gradient favors dendrite remelting through a local temperature or solute increases, which contribute to grain refinement [10]. Therefore, investigation of the dendrite growth characteristics of continuously cast steel is helpful to understand the formation mechanism of solidification defects and improve the solidification quality of steel. It has been proved that electromagnetic stirring has a large effect on billet quality by decreasing characteristic grain size, modifying columnar to equiaxed transition, reducing the defects of center segregation, porosities, and minimizing cracks [11–15].

In the present research, rotational electromagnetic stirring (R-EMS) combined with intensive cooling was applied in continuous casting of GCr15 bearing steel. The macrostructure, microstructure, and segregation of GCr15 bearing steel were investigated. This leads to a clearer understanding of the dendrite growth characteristics and helps to produce high-quality GCr15 bearing steel by continuous casting.

Experimental

The GCr15 bearing steel is prepared by continuous casting in the present research. Chemical analysis shows that the billet contains 0.98 wt% C, 0.20 wt% Si, 0.30 wt% Mn, 0.03 wt% P, 0.03 wt% S, 1.48 wt% Cr, and the balance is Fe. Figure 1 shows the schematic representation of the electromagnetic continuous casting system. The R-EMS was placed 0.6 m away from the bottom of the mould, as shown in Figure 1(3). The experimental conditions and operating parameters are shown in Table 1. The experiments were carried out without and with R-EMS, and the current intensity of R-EMS is 250 A, 350 A, respectively. In order to investigate the effect of cooling rate on solidification structure, the flow rate of the cooling water applied in the experiments is 2.0 m^3/h, 3.5 m^3/h (as shown in Figure 1(4)), respectively.

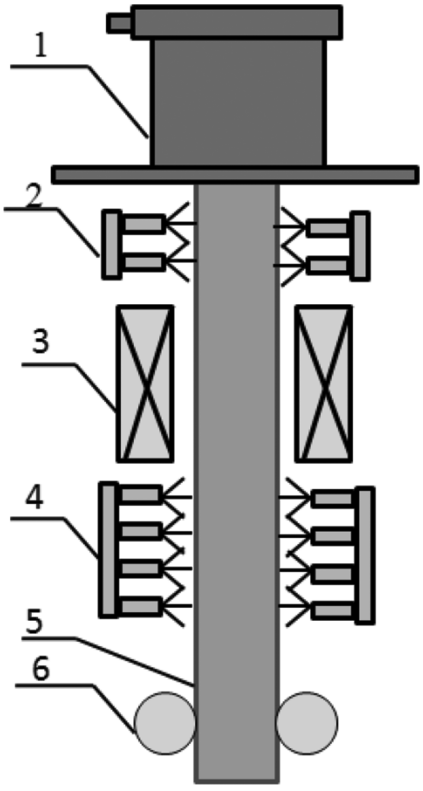

Figure 1: Schematic representation of the continuous casting system (1) mould, (2) upper water spray system, (3) R-EMS, (4) lower water spray system, (5) billet, (6) roller.

Table 1: Processing parameters applied in continuous casting.

Cross-sectional size (mm)	Casting speed (m/min)	Degree of superheat (K)	R-EMS current (A)	R-EMS frequency (Hz)
100 ×100	0.6	40	10, 250, 350	12

The transverse section specimens were collected for macrostructure inspection by chemically etched with a solution of 1 g $FeCl_3$, 5 g picric acid, 50 ml C_2H_5OH, and 50 ml H_2O. The microstructure morphology was investigated by using the OLYMPUS SZX16 microscope. The central regions of the billets were fractured and the fractured surfaces were observed by JSM-7100F scanning electron microscopy (SEM). Slices at different positions on the cross-sectional samples were collected using a drill of a diameter of 5 mm at intervals of 10 mm, and chemically analyzed by a Leco CS844 carbon sulfur analyzer.

Results

Effect of R-EMS on macrostructure

Figure 2 shows the cross-sectional macrostructures of the billets. Without R-EMS, the macrostructures are characterized by coarse columnar grains and developed cross dendrites (Figure 2(a)). The equiaxed crystal ratio is only 5 %, and there are crack and cavity in the center of the billet (Figure 3(a)). After applying R-EMS at 250 A, the crack and cavity disappear, but there are still developed cross dendrites in the center of the billet (Figures 2(b) and 3(b)). When the stirring current is 350 A, the internal quality of the billet is further improved, but a white band appears in the billet (Figures 2(c) and 3(c)). When the cooling water flow rate is increased from 2.0 m^3/h to 3.5 m^3/h, and applies R-EMS at 250 A, the macrostructures of the billet are dominated by fine columnar and equiaxed grains (Figures 3(d) and 4(d)), and the equiaxed crystal ratio is increased to 45 % (Figure 3(d)). The longitudinal macrostructures indicate consistent results with the cross-sectional macrostructures (Figure 3). The experimental results show that the billet quality is significantly improved when the stirring current is 250 A, and the cooling water flow rate is 3.5 m^3/h.

Effect of R-EMS on dendrite growth

To reveal the dendrite morphology characteristics of the solidifying structure, the dendrite morphologies at different solidification stages without and with R-EMS were investigated. With respect to the sample without

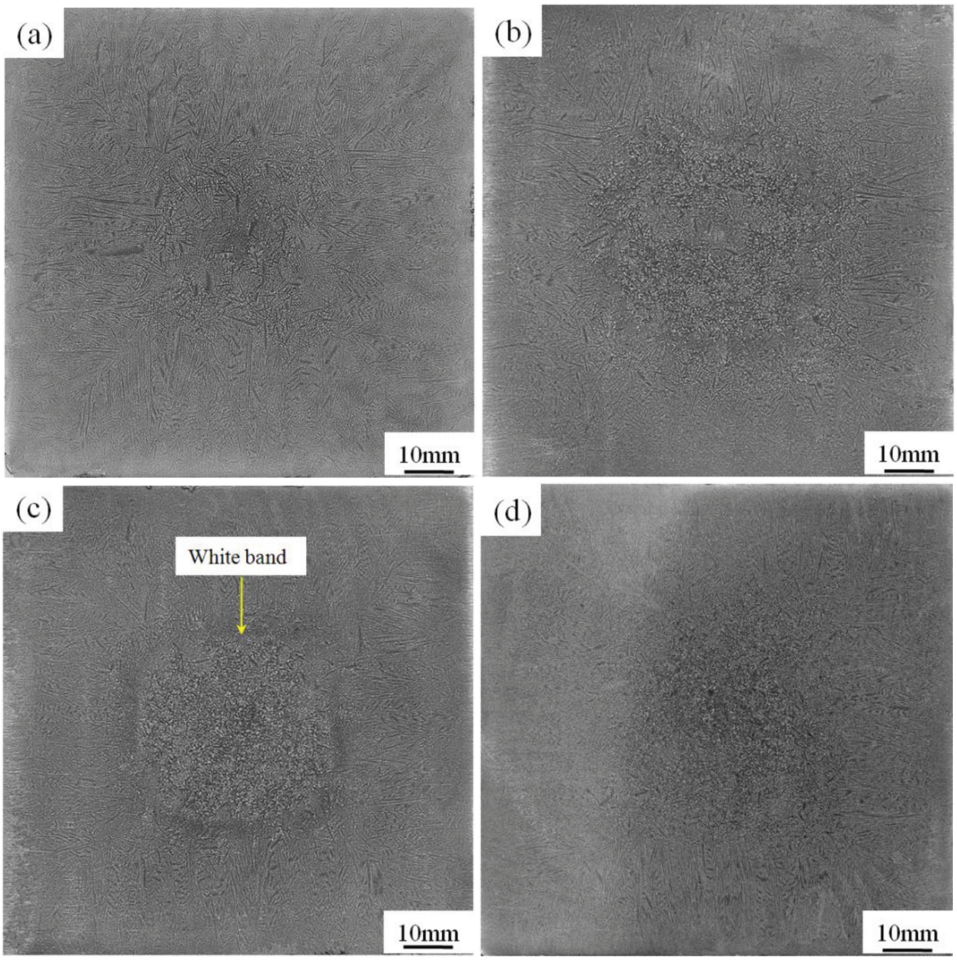

Figure 2: Cross-sectional macrostructures of acid etched samples solidified (a) without R-EMS, and with R-EMS (b) (cooling water flow rate Q is 2.0 m^3/h)), (c) 350 A (Q is 2.0 m^3/h), and (d) 250 A (Q is 3.5 m^3/h).

R-EMS, the columnar crystals are extremely slender and with a few branches, and almost grow towards one direction because of the large temperature gradient close to the solidified shell (Figure 4(a)). With the evolvement of solidification, the columnar crystals become shorter and coarser with no obvious orientation, and exhibit more and more crossed dendrites. Furthermore, the cavity and crack are observed in the center of the billet (Figure 4(b)). After applying R-EMS at 250 A, and the cooling water flow rate is 2.0 m^3/h, with the increasing flow intensity of the melt in front of the dendrite, the columnar dendrites intersect with each other and grow into cross dendrites, the solidification structure transforms from columnar dendrites to equiaxed dendrites (Figure 4(c) and (d)). When the cooling water flow rate is increased to 3.5 m^3/h, there are finely dispersed and compact equiaxed dendrites in the center of billet (Figure 4(e)). Meanwhile, the dendrite fragments are found in the billet with R-EMS (Figure 4(f)). Figure 5 shows the micro-morphologies of the central region by SEM. There are sharp dendrites in the porosity of the billet without R-EMS (Figure 5(a)). However, after applying R-EMS at 250 A, the sharp dendrites disappear, and the dendritic tips are more round (Figure 5(b)and (c)).

The secondary dendrite arm spacing (SDAS) is also investigated. It is clear shown that the SDAS in the same position is remarkably decreased when the R-EMS is applied (Figure 6). When the cooling water flow rate is increased from 2.0 m^3/h to 3.5 m^3/h with R-EMS, the SDAS is also slightly decreased. Meanwhile, the SDAS of dendrite fragments observed is approximately 160 μm, similar to without R-EMS in the region of Figure 5(a), and the length of dendrite fragments is approximately 1.5 mm, 7–10 times the SDAS. Therefore, R-EMS can change the morphology of dendrite, promote columnar-equiaxed transition, produce dendrite fragments, and decrease the secondary dendrite arm spacing.

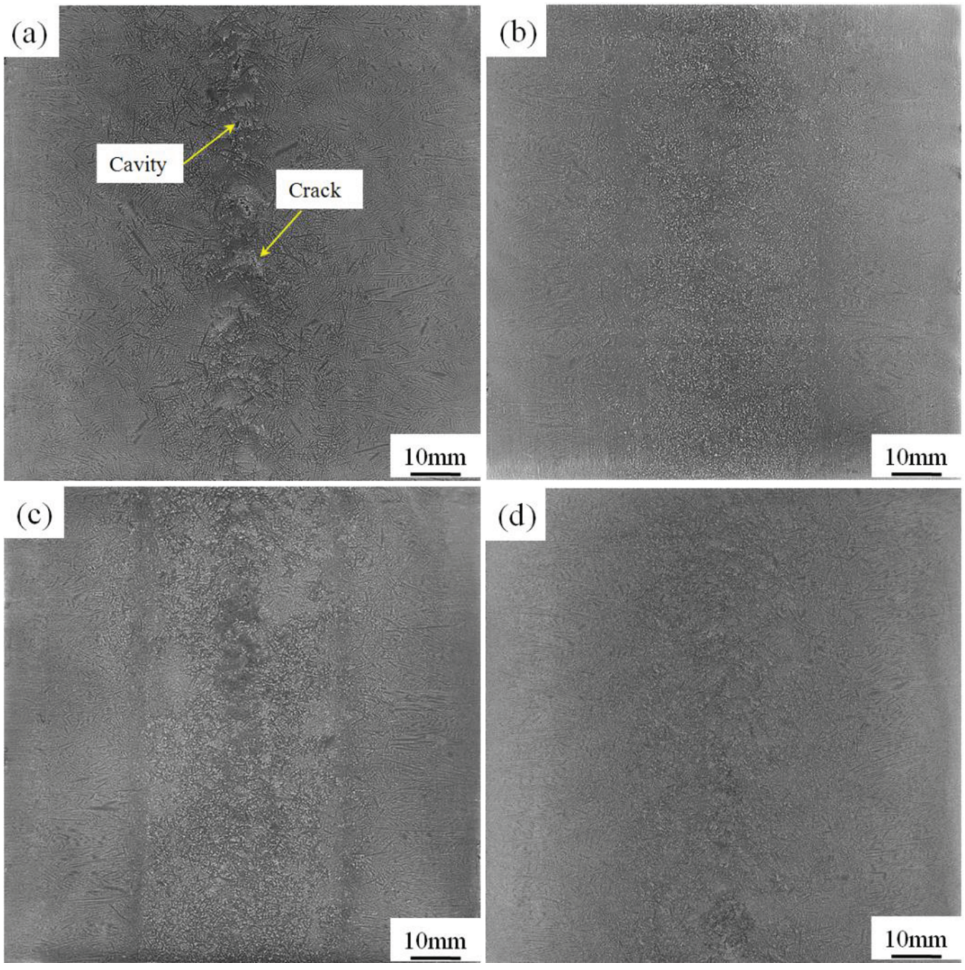

Figure 3: Longitudinal macrostructures of acid etched samples solidified (a) without R-EMS, and with R-EMS (b) 250 A (Q is 2.0 m^3/h), (c) 350 A (Q is 2.0 m^3/h), and (d) 250 A (Q is 3.5 m^3/h).

Effect of R-EMS on segregation

The billets without R-EMS and with R-EMS (the cooling water flow rate is 3.5 m^3/h) were compared to understand the effect of R-EMS on the segregation of sulfur and carbon. The centerline element segregation index K is expressed as a ratio of element analysis of the centerline to the averaged element analysis of the billet. Figure 7 shows there are carbon and sulfur positive segregation in the center of the billet without R-EMS. After applying R-EMS, both carbon and sulfur segregation have an obvious improvement. Figure 8 shows the SEM linear scanning results of carbon distribution along the central of the billet. Linear scanning the zones in the sample without R-EMS (Figure 8(a)) shows that carbon segregation is seen in the center rather than other positions. Scanning that with R-EMS (Figure 8(b) and (c)), however, show that more uniform carbon distribution and less segregation can be obtained. Therefore, R-EMS is beneficial to homogenize the distributions of both carbon and sulfur.

Discussion

The constitutional undercooling has been regarded as the most important factor influencing grain nucleation and growth [16]. According to the constitutional undercooling criterion [17]:

$$\frac{G_L}{R} \le \sum_{i=1}^{n} \frac{m_{L,i} c_{o,i} (k_{o,i} - 1)}{D_{L,i} k_{o,i}} \tag{1}$$

where G_L is the actual temperature gradient in the liquid, $R$is the growth rate, $m_{L,i}$ is the slope of the liquidus line in the phase diagram of the Fe-i system, $c_{o,i}$is the equilibrium partition coefficient of solute i, and $D_{L,i}$ is the

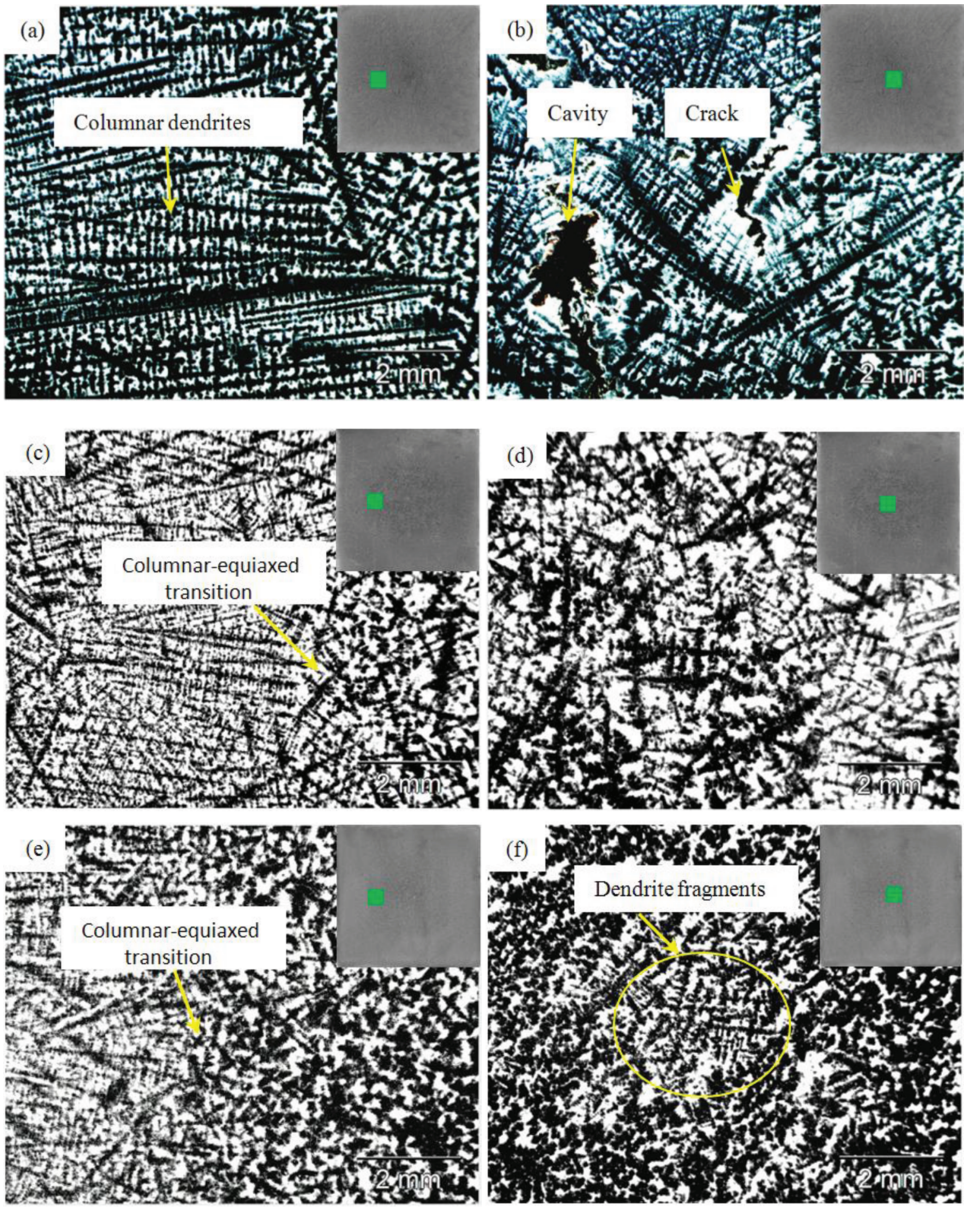

Figure 4: Dendrite morphology of the billets: (a, b) without R-EMS, (c, d) with R-EMS (Q is 2.0 m^3/h), (e, f) with R-EMS (Q is 3.5 m^3/h).

diffusion coefficient of solute*i* in liquid steel. The temperature gradient G_L can effectively influence the type of grain morphology. Due to the high temperature gradient at the interface without R-EMS, the solidification structure is characterized by coarse columnar grains and developed cross dendrites. Applying R-EMS, the forced convection makes the uniform distribution of temperature and concentration fields so as to decrease the $G_L$ahead of the solidification front. As shown in eq. (1), the smaller the temperature gradient, the easier the constitutional undercooling occurs, and it will be beneficial to convert the solidification structure from columnar crystals to equiaxed crystals. On the other hand, the temperature and solutes at the end fields of the primary phase particles and the secondary dendrite arm tips tend to get a uniform distribution. It will prevent the rapid growth of the dendrite backbone and decrease the dendrite arm spacing [18]. In addition, increasing the cooling water flow rate from 2.0 m^3/h to 3.5 m^3/h where the billet just come out the stirrer, can enhance the heat transfer from the central to the surface, and accelerate the dissipation of steel overheat, which can enhance the nucleation ratio and refine the structure.

Furthermore, dendrite fragments are found in the billet with R-EMS. The circular flow of molten steel produces a shear stress on the growing dendrite. If the

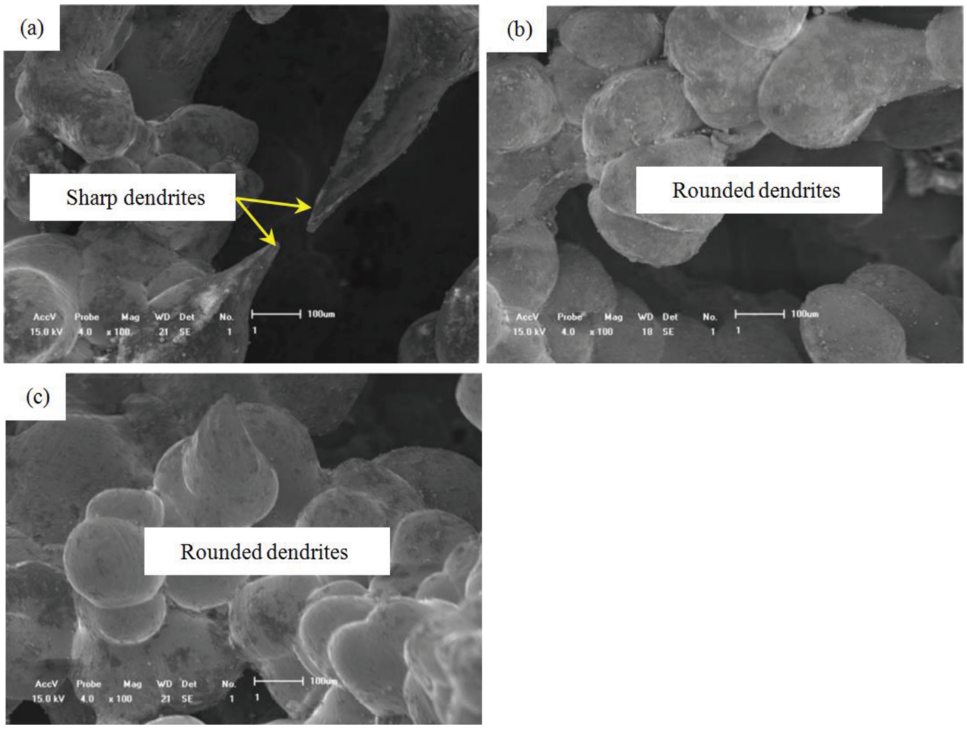

Figure 5: Microstructural morphologies of central region in the samples (a) without R-EMS and with R-EMS (b) 250 A (Q is 2.0 m^3/h), (c) 250 A (Q is 3.5 m^3/h).

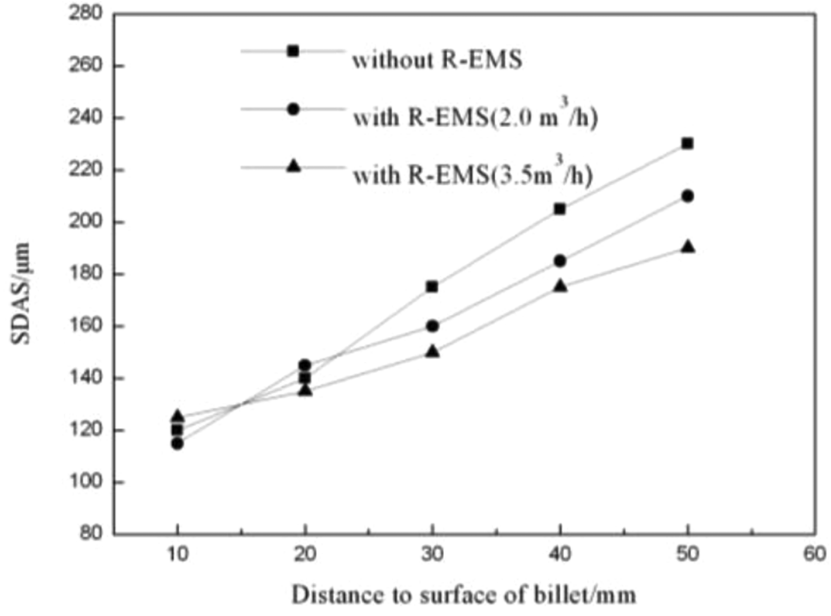

Figure 6: Variations of the secondary dendrite arm spacing (SDAS) with the distance from the edge to the center of specimen.

shear stress exceeds the ultimate strength, the growing dendrite at the solidification front will be broken. Meanwhile, the circular flow takes overheated molten steel into the mushy zone, and the ultimate strength of growing dendrite decreases with the increasing temperature. Therefore, the breakage of growing dendrites becomes easier. Then, some dendrite fragments detach from growing columnar dendrites and drift from the mushy zone to the center zone if they satisfy following criterion [19]:

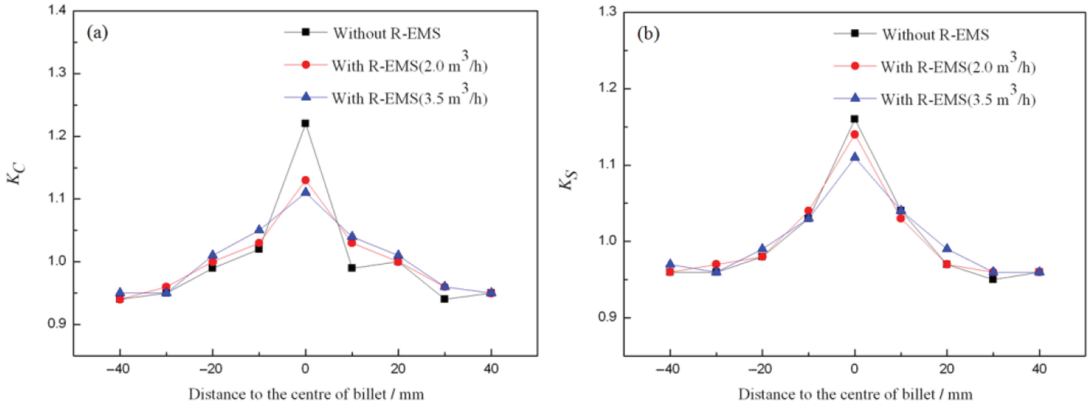

Figure 7: Centerline segregation index of (a) carbon and (b) sulfur at different positions of the samples with and without R-EMS.

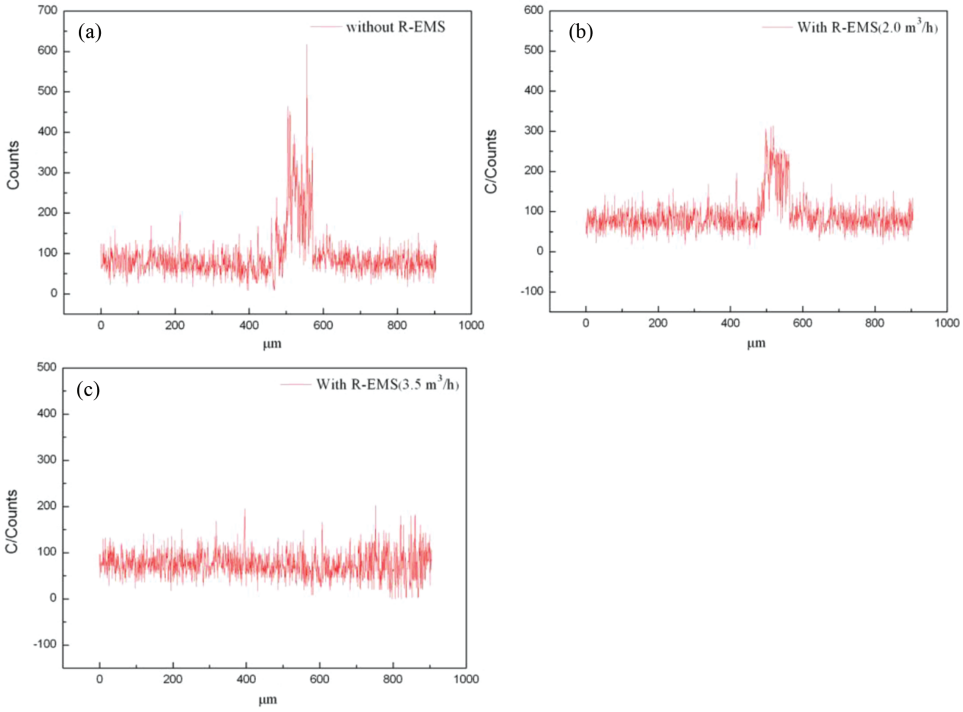

Figure 8: The distributions of carbon collected from linear scanning along the central of the billet (a) without R-EMS and with R-EMS of (b) 250 A (Q is 2.0 m^3/h), and (c) 250 A (Q is 3.5 m^3/h).

$$C_R = \frac{u_{l,z}^d}{V_C} > 1 \tag{2}$$

where $u_{l,z}^d$ is the local fluid velocity u_l^dprojection on the thermal gradient, $V_C$is the solidification speed. The dendrite fragments disperse in the liquid steel, and some fragments can partially remelt to become more effective nuclei. All the effects can effectively refine the microstructure and broaden the equiaxed zone.

Conclusion and future work

The main conclusion can be summarized as follows:

(1) With effect of R-EMS (stirring current of 250 A and the cooling water flow rate is 3.5 m^3/h), the macrostructure of the billet is refined. The fraction of the equiaxed grain is increased from 5 % to 45 %, the secondary dendrite arm spacing is decreased, and

the center segregations of both carbon and sulfur are reduced as well.

(2) Applying R-EMS, dendrite fragments are found in the vicinity of the center region, 7–10 times the SDAS. Some fragments can partially remelt to become effective nuclei, and some fragments survive the solidification process.

Future work will focus on the experiment research regarding to which is the key mechanism for the origin of equiaxed grains between constitutional undercooling and remelting-induced fragmentation.

Funding: This work was financially supported by the National Nature Science Foundation of China (No. 50834009), the Key Project of the Ministry of Education of China (No. 311014), and the Programme of Introducing Talents of Discipline to Universities (the 111 Project of China, No. B07015).

References

[1] J.W. Fu, Appl. Phys. A, 122 (2016) 416–421.
[2] H. Sun, L. Li and X. Cheng, Ironmaking Steelmaking, 42 (2015) 439–449.
[3] J. Guo, D.S. Qian and J.D. Deng, J. Mater. Process. Tech., 231 (2016) 151–161.
[4] S.O. Kyung and W.C. Young, ISIJ Int., 35 (1995) 866–875.
[5] C. Xiao, J.M. Zhang and Y.Z. Luo, J. Iron Steel Res. Int., 20 (2013) 13–20.
[6] M. Yamazaki, Y. Natsume, H. Harada and K. Ohsasa, ISIJ Int., 46 (2006) 903–908.
[7] Z.B. Hou, F. Jiang and G.G. Cheng, ISIJ Int., 52 (2012) 1301–1309.
[8] S. Luo, M.Y. Zhu and S. Louhenkilpi, ISIJ Int., 52 (2012) 823–830.
[9] Y. Natsume, D. Takahashi, K. Kawashima and K. Matsuura, ISIJ Int., 53 (2013) 838–847.
[10] S. Liu, S.-Z. Lu and A. Hellawell, J. Cryst. Growth, 234 (2002) 740–750.
[11] H.J. Wu, N. Wei and Y.P. Bao, Int. J. Miner. Metall. Mater., 18 (2011) 159–164.
[12] L. Bettlman, Can. Metall. Q., 38 (1999) 301–309.
[13] K.S. Oh and Y.W. Chang, ISIJ Int., 35 (1995) 866–875.
[14] M. Raj and J.C. Pandey, Ironmaking Steelmaking, 35 (2008) 288–296.
[15] Y. Xu, R.J. Xu and Z.J. Fan, Int. J. Miner. Metall. Mater., 23 (2016) 534–541.
[16] P. Lan, H. Tang and J.Q. Zhang, Metall. Mater. Trans. A, 47A (2016) 2964–2984.
[17] W.A. Tiller, K.A. Jackson, J.W. Rutter and B. Chalmers, Acta Metall., 1 (1953) 428–437.
[18] J.M. Cabrera-Marrero, V. Carreño-Galindo and R.D. Morales, ISIJ Int., 38 (1998) 812–821.
[19] T. Campanella, C. Charbon and M. Rappaz, Metall. Mater. Trans. A, 35A (2004) 3201–3210.